

Short Communication

Preparation of Magnetic Iron/Graphitic Mesoporous Carbon Composites as Efficient Returnable Adsorbents for Methyl Orange Removal

Lifeng Cui^{1,*}, Mingcui Yao², Xia Bai², Lu Zhang², Shifei Kang^{2,*}

¹ School of Chemistry and Environmental Engineering, Dongguan University of Technology, Guangdong 523808, P. R. China.

² Department of Environmental Science and Engineering, University of Shanghai for Science and Technology, Shanghai 200093, China

*E-mail: lifeng.cui@gmail.com, sfkang@usst.edu.cn

Received: 24 June 2016 / Accepted: 8 August 2016 / Published: 6 September 2016

The mesoporous silica SBA-15 was regarded as the template to synthesize a variety of magnetic iron/graphitic mesoporous carbon (Mag-GMC) composites, via a simple one-step solid-liquid grinding/templating route. The physicochemical properties of these composites were characterized by X-ray diffractometry, nitrogen sorption isotherms, transmission electron microscopy and vibrating-sample magnetometry. The methyl orange (MO) removal effects of these composites as adsorbents were investigated via a batch adsorption technique, and the effects of contact time and initial MO concentration on the adsorption capacity were also discussed. Also, the zeta potential of the as-prepared Mag-GMC composites was measured and compared. Mag-GMC-0.5 shows the highest MO adsorption ability of 90.6 mg/g, which is much higher than that of commercial active carbon. Recycle adsorption experiments indicate that the Mag-GMC composites are promising in returnable dye removal. The excellent adsorption performance can be ascribing to its unique mesoporous structure and decent zeta potential.

Keywords: Magnetic materials, Graphitic mesoporous carbon, Adsorption, Dye removal, zeta potential

1. INTRODUCTION

Currently, dye staffs are commonly used in various industries, including textile, food, printing, pharmaceutical, leather, cosmetic and paper industries. Since the dyeing technique was invented, however, a large number of colored wastewater has been discharged into the environment [1-3]. Most

of dyes are recalcitrant molecules (particularly azo dyes) and recognized to be of synthetic origin and toxicity. The complex composition, chemical stability and high chemical oxygen consumption make these dyes refractory, thus inducing potential carcinogenic and genotoxic effects [4,5]. Therefore, dye removal becomes a very important but challenging area of wastewater treatment [6]. The conventional dye removal methods have some limitations, such as inefficiency at low concentrations, large need of chemicals and energy, and prohibitively high cost [7]. Hence, from the perspective of environmental protection, developing a sustainable competitive effluent management method for the dyeing industry has long been an important task.

Recently, there exists a most appropriate and convenient method for removal of different dyes for the adsorption process in which we use lower cost adsorbents. In this regard, researchers attached most attention on various commercial adsorbents, for example, granular activated carbon [8,9], molecular sieve [10,11], activated diatomite [12,13], and resins [14,15]. However, when most of the adsorbents are to be separated from treated solutions, traditional methods such as filtration and sedimentation may block the filters or induce the loss of adsorbent and cause secondary pollution [16]. Recently, the magnetic adsorption techniques, due to their convenience, rapidness, low cost and amenability to automation methods [17], have received considerable attention [18], while magnetically separable mesoporous carbon composites are an efficient choice to overcome the above-mentioned problems [19]. Therefore, ferromagnetism species were introduced into mesoporous carbon materials to prepare magnetic mesoporous carbon composites, which are promising adsorbents for separation of dyes from solutions [20-23]. To the best of our knowledge, however, their extensive applications in the separation procedure are limited by the low saturated magnetization strength and poor stability.

Herein, we prepared the Mag-GMC composites through a simple procedure, in which we can observe the decentralization of high contents of magnetic iron nanoparticles. In the synthesis, ordered mesoporous silica SBA-15 was regarded as a mesoporous template, soybean oil was used as a carbon source, as well as $\text{FeCl}_3 \cdot 6\text{H}_2\text{O}$ as an iron precursor. As one of the most prominent advantages, the operation and enlargement of this method is easy. Moreover, the structural properties of the Mag-GMC composites as-obtained were analyzed by X-ray diffractometry (XRD), nitrogen adsorption-desorption isotherms, transmission electron microscopy (TEM) and vibrating-sample magnetometry (VSM). Meanwhile, to detect the procedure of the decolorization of synthetic wastewater containing MO which is a widely-used azo dye, we also investigated their adsorption capacities.

2. EXPERIMENTAL

The Pluronic triblock copolymers (P123, EO20PO70EO20, Mw = 5800) was purchased from Sigma-Aldrich Co., LTD.. Tetraethoxysilane (TEOS), HCl, glycerol, NaOH and $\text{FeCl}_3 \cdot 6\text{H}_2\text{O}$ were purchased from Sinopharm Chemical Reagent Limited Corporation. Soybean oil was obtained from a Shanghai Lotus supermarket. All chemicals in the study were of analytically pure grade and used without further purification. SBA-15 with rod-like morphology was fabricated in accordance with per previous report [22], but with one difference that the amount was amplified by ten times. Mag-GMC composites were prepared via a one-step solid-liquid grinding/templating route. In a typical process,

SBA-15, soybean oil, and $\text{FeCl}_3 \cdot 6\text{H}_2\text{O}$ at the weight ratio of 1:2: x ($x = 0$ to 1.5) was carbonized at 900 °C under N_2 flow for 5 h, and then SBA-15 was removed by addition of 2 M NaOH aqueous solution. We prepared a range of Mag-GMC composites with different magnetic iron contents and denoted as Mag-GMC- x (x denotes the amount of iron salt).

The crystalline structures and compositions of the Mag-GMC composites were identified by a θ - 2θ mode of a Bruker D8 Advance XRD meter with $\text{Cu K}\alpha_1$ radiation ($\lambda = 1.5406 \text{ \AA}$), operated at 40 kV and 40 mA (scanning step: $0.02^\circ/\text{s}$). TEM images were taken using a JEOL JEM-2010 TEM device with an acceleration voltage of 200 kV. Nitrogen sorption isotherms were measured at 77 K on a BeiShiDe Instrument, a 3H-2000PS4 Specific Surface & Pore Size Analyzer. VSM measurements were performed by using a VSM meter (Lake Shore 7410 VSM). The value of the zeta potential and diameter distribution of the samples was determined using Laser Zeta meter Malvern Instruments (Zetasizer Nano ZS 90) in water solution (PH=7.4).

The adsorption experiments were carried out under unified conditions in incubator shakers. Typically, 50 mg magnetic iron/graphitic mesoporous carbon composites and 50 mL Methyl Orange stock solutions of different concentration were mixed and oscillated fully for about 4 hours at 25 °C, after which the mixture was centrifuged for 10 min. The absorbance of the obtained supernatants was measured using a 752 type spectrophotometer at wavelength 461.0 nm to determine the removal effect of Mag-GMC composites for MO dye.

3. RESULTS AND DISCUSSION

Nitrogen sorption isotherms were recorded to investigate how iron contents affected the pore properties of the composites. The pore size distribution was determined by analyzing the desorption branch of the isotherms.

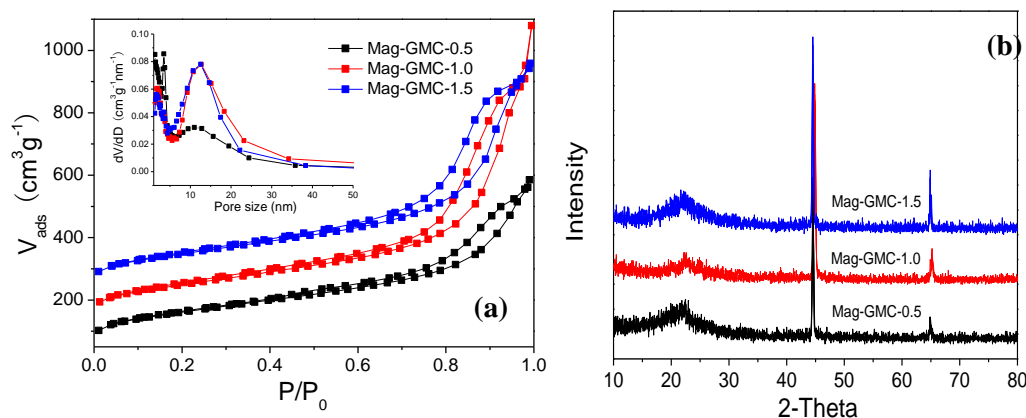


Figure 1. (a) Nitrogen adsorption-desorption isotherms and (b) XRD patterns of Mag-GMC-0.5, Mag-GMC-1.0, and Mag-GMC-1.5; the pore size distribution curves are showed in the inset in (a).

The nitrogen sorption isotherms of Mag-GMC-0.5, Mag-GMC-1.0 and Mag-GMC-1.5 were shown in Figure 1a, as well as their corresponding pore size distribution curves (inset in Figure 1a). Clearly, due to the capillary condensation, three isotherm curves all show a strong N_2 uptake in a wide range of relative pressure (P/P^0 , 0.40–0.95), which indicates the existence of multiform pore distributions. Clearly, these Mag-GMC composites all possess uniform bimodal pore size distributions centered at about 3.3 and 12.3 nm, and we regard it as the causes of the dissolution of silica walls and the coalescence of unfilled spaces of SBA-15. Together with the TEM image below, pores can be divided into ordered and disordered types, which result from the wide dispersion of the precursor inside and outside of the hard template, respectively, during the incorporation. The Brunauer-Emmett-Teller (BET) surface areas of these hierarchical Mag-GMC composites generally are as large as 526.6–564.4 m^2/g and the pore volumes are also as large as 0.905–1.515 cm^3/g , which may endow the adsorbents with high adsorption capacity. The crystallinity and phase components of the samples were examined by powder XRD (Fig. 1b). In the above figure.1b, there exists a relatively broad peak at around 25° which indexes the (0 0 2) reflection for graphitic carbon [25-27]. The intense peaks at about 44° and 65° can be well indexed to pure α -Fe, but no evidence of iron oxide can be observed. What should be remarked is that we can ascribe an overlapped strong (1 1 0) reflection of α -Fe to the (1 0 1) reflection from graphitic carbon disappears. As the content of iron salts increases, the peaks of α -Fe become stronger, indicating the increased amount of magnetic iron particles.

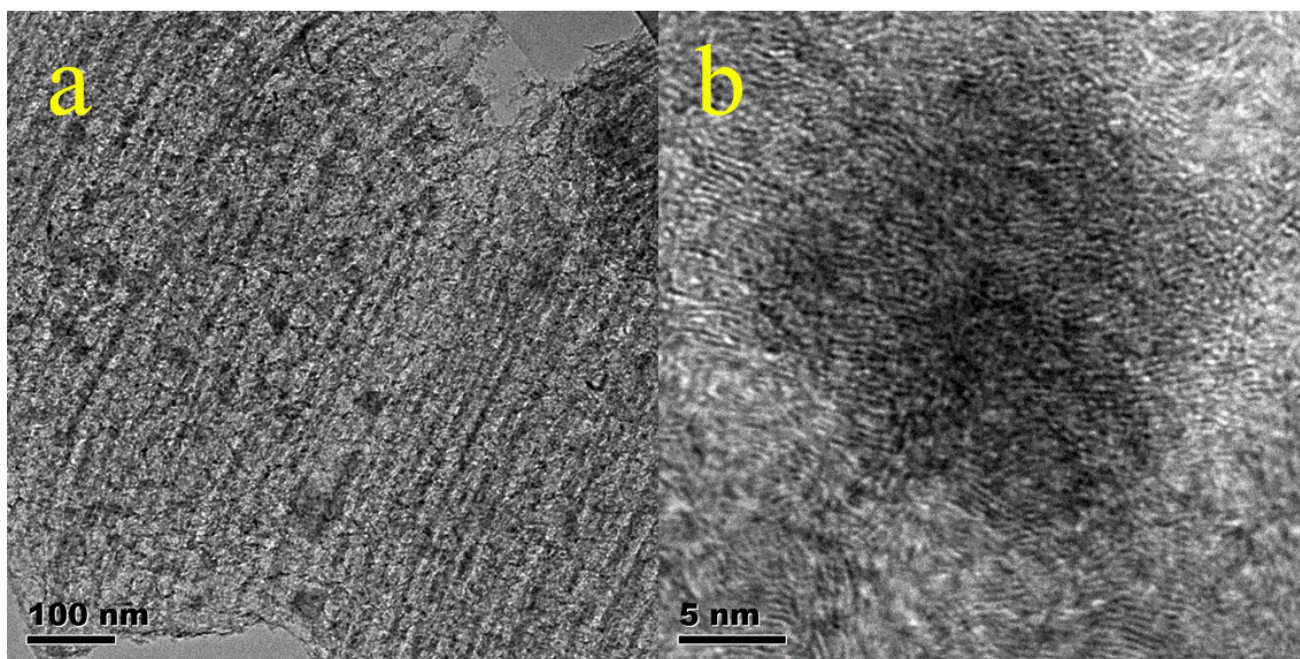


Figure 2. (a) TEM and (b) HRTEM images of Mag-GMC-1.0

The low-resolution TEM of the representative Mag-GMC-1.0 (Fig. 2a) exhibits no evident large magnetic iron particles. The phenomenon that nano-sized iron particles are homodispersed in the GMC shows that ordered 2D hexagonal mesostructured formed a large area. The sizes of most

nanoparticles are similar to the diameter of the carbon rods, which is similar to the channel size of SBA-15. The dark magnetic iron nanocrystals whose sizes is between 5 and 7 nm, which are more evident in the high-resolution TEM (HRTEM) image (Fig. 2b), are well embedded in the GMC walls. No bulk aggregates appear on the external surface of the mesoporous carbons, indicating that the materials are suitable for separation of dyes.

The magnetic properties of Mag-GMC-0.5, Mag-GMC-1.0 and Mag-GMC-1.5 samples were characterized by magnetic hysteresis loops in a varying magnetic field at room temperature. According to the magnetization curves, the magnetic properties of most iron nanoparticles can be identified are superparamagnetic. The corresponding saturation magnetization strengths (M_s) of Mag-GMC-0.5, Mag-GMC-1.0 and Mag-GMC-1.5 are 22.6, 29.1 and 38.9 emu/g, respectively, indicating that according to the increase of iron content, M_s is large enough to magnetic separation.

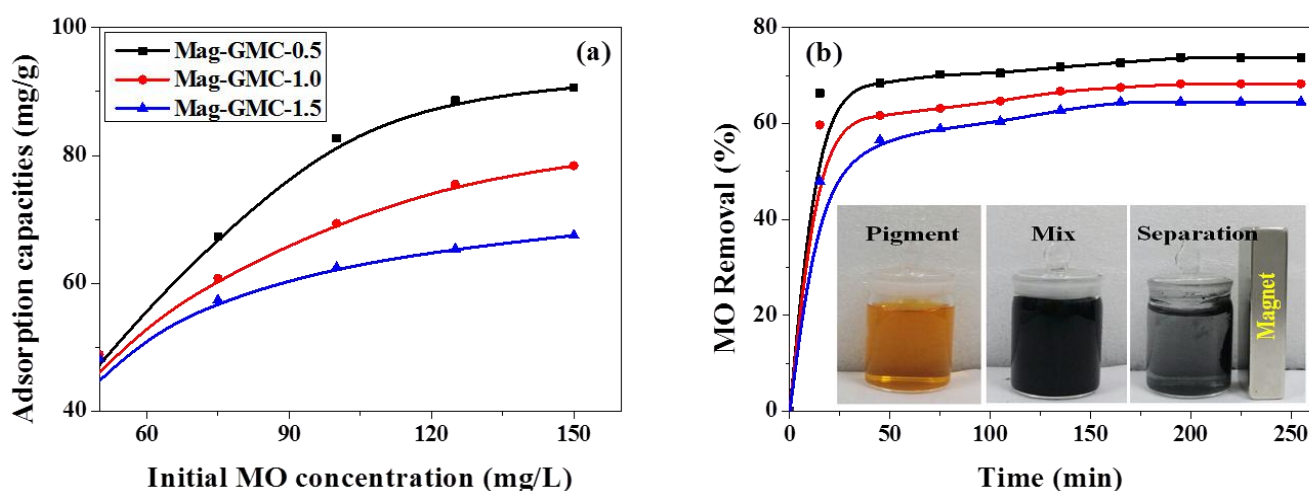


Figure 3. (a) Effect of initial MO concentration on dye removal and (b) the adsorption kinetics of MO onto the three composites. The inset in (b) shows the Mag-GMC-0.5 dispersed in MO solution before and after attraction by an outer magnet.

All the mesoporous carbon samples were tested in adsorption of MO, an organic compound that belongs to azo dyes containing $-N=N-$ as a chromophore [3]. Effect of initial MO concentration (from 50 to 150 mg/L) on adsorption was tested (Fig. 3a). Clearly, the adsorbed amounts of dye molecules on the three composites increase quickly at the initial stages and then rise further but slowly. The corresponding adsorption capacities of Mag-GMC-0.5, Mag-GMC-1.0, and Mag-GMC-1.5 are 90.6, 78.4, as well as 67.5 mg/g, respectively, indicating that due to the increase of iron content, the adsorption capacity of the Mag-GMC composites is reduced correspondingly. It is suggested that hierarchical mesoporous structure plays a crucial role in the loading of biomolecules. The adsorption capacity of MO intensified with the increase of the MO concentration may be attributed to an enhancement in the driving force of concentration gradient [1]. Moreover, the time dependence of MO adsorption onto the Mag-GMC composites was investigated to determine the time required to reach the

solid-solution equilibrium. As shown in Fig. 3b, the three composites have similar plots and generally the same trend: adsorption is very rapid at the initial few minutes, and then slower down largely for a longer period. The equilibrium time is about 150 min for all the three composites. At the beginning, most of the dye molecules were first adsorbed onto the exterior surfaces of the adsorbent, which accelerates the adsorption rate. When the adsorption by the exterior surface was saturated, the dye molecules extended into the pores and were absorbed by the interior surfaces of the adsorbent.

In order to test the magnetic separating and recycling properties of such magnetic composites, we well dispersed Mag-GMC-0.5 in MO solution, forming a dark suspension without an outer magnet. After a conventional laboratory magnet was placed near the beaker, the mixture rapidly turned from black to colorless within a few minutes (inset of Fig. 3b). According to the simple experiment, we can obviously find that these Mag-GMC materials have significant potential and effectiveness that they can remove compounds in liquid phase and achieve a simple separation of absorbents and solution. Therefore, the Mag-GMC composites prepared here shows both good adsorption ability and outstanding magnetic separation performance compared with conventional activated carbon.

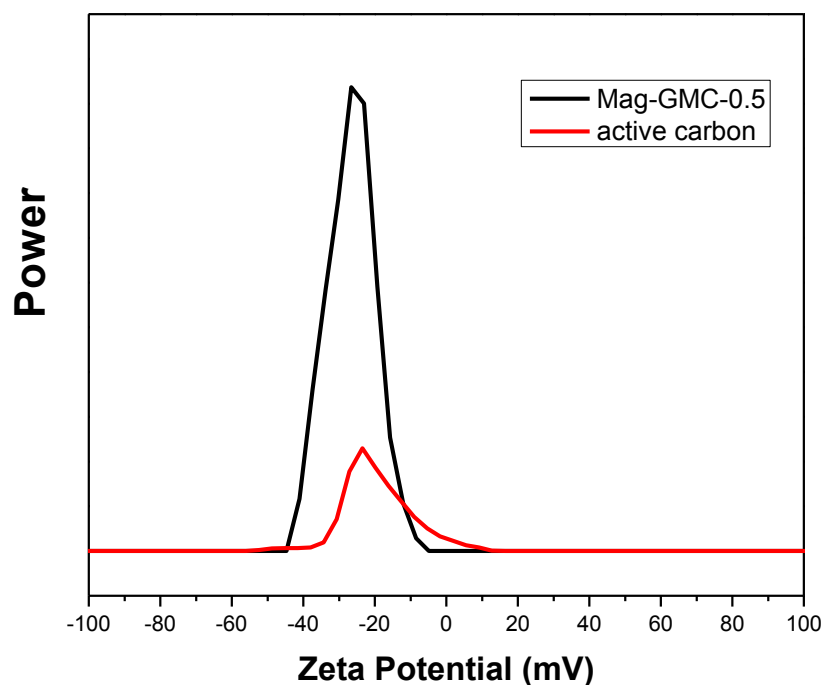


Figure 4. Zeta potential (mV) of Mag-GMC-0.5 and commercial active carbon in water (pH=7, 25 °C).

The zeta potential value, which can describes the nanomaterials distribution state and reflects the electrostatic interactions of soluble pollutants on the surfaces of adsorbent, is often used to evaluate the adsorption potential and character of dye molecules on the nanomaterials surfaces. In this respect, the zeta potential of Mag-GMC-0.5 and commercial active carbon samples was recorded in water (pH=7, 25 °C) as shown in Fig. 4. The calculated Zeta potential of Mag-GMC-0.5 is -26.6 mV, which is higher than that of active carbon (-16.9 mV), indicating the stability of colloidal systems of the Mag-GMC-0.5 dispersion in water is better than active carbon. The negative charges on the surface of Mag-GMC-0.5

in liquid dispersion are important for static interaction with cationic dye. Moreover, the dye pollutants removal efficiencies of Mag-GMC-0.5 can be increased because of lower zeta potential values. It is well known that zeta potential values higher than +30mV or lower than -30mV means a relatively stable suspensions state[28], the Mag-GMC-0.5 have zeta potential values very close to stable colloidal systems, this provide better dye removal potential , meanwhile the materials magnetic separating and recycling can be much easier than in typical stable suspensions. Therefore, the zeta potential of Mag-GMC-0.5 is quite suitable for adsorbent of dye stuffs.

In summary, the excellent returnable adsorption effect for MO removal can be ascribed to the unique structure and surface property of Mag-GMC composites, which allow magnetic nano-sized iron particles to be homodispersed in the GMC framework, thus providing enough adsorption interfaces and facilitating the durable magnetic recycling. Besides, the negative surface charge and decent zeta potential value further facelifted the adsorption removal of dye stuffs in water.

4. CONCLUSIONS

In conclusion, the magnetic Fe/GMC composites fabricated through a simple one-step solid-liquid grinding/templating way. The magnetic composites possess an ordered 2D hexagonal mesoporous structure. The considerable BET surface areas (526.6– 564.4 m²/g) and large pore volumes (0.905–1.515 cm³/g) was recorded, which endow the adsorbents with high adsorption capacity. The magnetic iron nanoparticles were confined in the matrix of the GMC frameworks, and the saturated magnetization strength of the composites was adjusted from 22.6 to 38.9 emu/g by increasing iron content. Because of enough adsorption interfaces providing by the unique bimodal pore systems and decent zeta potential value, the magnetic composites exhibit and excellent returnable adsorption effect for MO removal.

ACKNOWLEDGEMENTS

This work was supported by National Natural Science Foundation of China (Grant No.51528202 and 51502172), Capacity-Building of Local University Project by Science and Technology Commission of Shanghai Municipality (Grant No. 12160502400) and Program of Shanghai Pujiang Talent Plan (Grant No. 14PJ1406800).

References

1. I.A. Tan, A.L. Ahmad and B.H. Hameed, *J. Hazard. Mater.*, 154(2008)337.
2. Y. Bulut, N. Gözübenli and H. Aydın, *J. Hazard Mater.*, 144(2007)300.
3. J. Goscianska, M. Marciniak and R. Pietrzak, *Chem. Eng. J.*, 247(2014)258.
4. Y. Dong, H.M. Lin and F.Y. Qu, *Chem. Eng. J.*, 193-194(2012)169.
5. S. Chatterjee, S. Chatterjee, B.P. Chatterjee, A.R. Das and A.K. Guha, *J. Colloid Interface Sci.*, 288(2005)30.
6. Q.H. Hu, S.Z. Qiao, F. Haghseresht, M.A. Wilson and G.Q. Lu, *Ind. Eng. Chem. Res.*, 45(2006)733.
7. S. Mondal, *Environ. Eng. Sci.*, 25(2008)383.

8. K.D. Belaid, S. Kacha, M. Kameche and Z. Derriche, *J. Environ. Chem. Eng.*, 1(2013)496.
9. G.M. Walker, *Water Res.*, 31(1997)2093.
10. Y. Hu, Y.Y. He, X.W. Wang and C.H. Wei, *Appl. Surf. Sci.*, 311(2014)825.
11. M. Guan, W. Liu, Y.L. Shao, H.Y. Huang and H.X. Zhang, *Microporous Mesoporous Mater.*, 123(2009)193.
12. R.K. Sheshdeh, M.R.K. Nikou, K. Badii, N.Y. Limaee and G. Golkarnarenji, *J. Taiwan Inst. Chem. Eng.*, 45(2014)1792.
13. E. Erdem, G. Colgecen and R. Donat, *J. Colloid Interface Sci.*, 282(2005)314.
14. S. Karcher, A. Kornmuller and M. Jekel, *Water Res.*, 36(2002)4717.
15. M. Wawrzkievicz, *Chem. Eng. J.*, 217(2013)414.
16. D.H.K. Reddy and S.M. Lee, *Adv. Colloid Interface Sci.*, 201-202(2013)68.
17. A.M. Donia, A.A. Atia and K.Z. Elwakeel, *J. Hazard Mater.*, 151(2008)372.
18. D. Hritcu, D. Humelnicu, G. Dodi and M.I. Popa, *Carbohydr. Polym.*, 87(2012)1185.
19. J. Liu, S.Z. Qiao, Q.H. Hu and G.Q. Lu, *Small*, 7(2011)425.
20. Z.L. Wang, X.J. Liu, M.F. Lv and J. Meng, *Carbon*, 48(2010)3182.
21. Y.P. Zhai, Y.Q. Dou, X.X. Liu, B. Tu and D.Y. Zhao, *J. Mater. Chem.*, 19(2009)3292.
22. Y.G. Wang, F.Y. Zhang, Y.Q. Wang, J.W. Ren, C.L. Li, X.H. Liu, Y. Guo, Y.L. Guo and G.Z. Lu, *Mater. Chem. Phys.*, 115(2009)649.
23. S.Y. Dai, S.Y. Yang and D.Q. Zhou, *Int. Conf. Electr. Eng. Autom. Control*, 12(2010)206.
24. B. Tanhaei, A. Ayati, M. Lahtinen and M. Sillanpää, *Chem. Eng. J.*, 259(2015)1.
25. Y.G. Wang, C.L. Zhang, S.F. Kang, B. Li, Y.Q. Wang, L.Q. Wang and X. Li, *J. Mater. Chem.*, 21(2011)14420.
26. Y. Tian, P. Liu, J. Wang, X.F. Wang and H.S. Lin, *Mater. Lett.*, 82(2012)19.
27. G.X. Li, Y.X. Guo, X. Sun, T. Wang, J.H. Zhou and J.P. He, *J. Phys. Chem. Solids*, 73(2012)1268.
28. H. Sun, J. Yu, P. Gong, D. Xu, C. Zhang, S. Yao, *Journal of Magnetism and Magnetic Materials* 294 (2005) 273–280.